

RESEARCH ARTICLE

Open Access

# Hippocampal expression of murine IL-4 results in exacerbation of amyloid deposition

Paramita Chakrabarty<sup>1</sup>, Li Tianbai<sup>1</sup>, Amanda Herring<sup>1</sup>, Carolina Ceballos-Diaz<sup>1</sup>, Pritam Das<sup>2</sup> and Todd E Golde<sup>1\*</sup>

## Abstract

**Background:** Pro-inflammatory stimuli, including cytokines like Interleukin-1 $\beta$ , Interleukin-6 and Interferon- $\gamma$ , in the brain have been proposed to exacerbate existing Alzheimer's disease (AD) neuropathology by increasing amyloidogenic processing of APP and promoting further A $\beta$  accumulation in AD. On the other hand, anti-inflammatory cytokines have been suggested to be neuroprotective by reducing neuroinflammation and clearing A $\beta$ . To test this hypothesis, we used adeno-associated virus serotype 1 (AAV2/1) to express an anti-inflammatory cytokine, murine Interleukin-4 (mIL-4), in the hippocampus of APP transgenic TgCRND8 mice with pre-existing plaques.

**Results:** mIL-4 expression resulted in establishment of an "M2-like" phenotype in the brain and was accompanied by exacerbated A $\beta$  deposition in TgCRND8 mice brains. No change in holo APP or APP C terminal fragment or phosphorylated tau levels were detected in mIL-4 expressing CRND8 cohorts. Biochemical analysis shows increases in both SDS soluble and insoluble A $\beta$ . mIL-4 treatment attenuates soluble A $\beta$ 40 uptake by microglia but does not affect aggregated A $\beta$ 42 internalization by microglia or soluble A $\beta$ 40 internalization by astrocytes.

**Conclusions:** Short term focal mIL-4 expression in the hippocampus leads to exacerbation of amyloid deposition in vivo, possibly mediated by acute suppression of glial clearance mechanisms. Given that recent preclinical data from independent groups indicate engagement of the innate immune system early on during disease pathogenesis may be beneficial, our present study strongly argues for a cautious re-examination of unwarranted side-effects of anti-inflammatory therapies for neurodegenerative diseases, including AD.

**Keywords:** Interleukin 4, Inflammation, Adeno-associated virus, Hippocampus, Amyloid plaque, Amyloid precursor protein

## Background

Amyloid  $\beta$  (A $\beta$ ) plaques constitute a hallmark pathological feature of Alzheimer's disease (AD), the most prevalent neurodegenerative disorder. Neuroinflammation has been hypothesized to play a pathogenic role in the development of sporadic AD, particularly because pro-inflammatory cytokines and chemokines colocalize with neurodegenerative pathology in both AD patient brains as well as in transgenic mouse models of AD type pathology (reviewed in [1]). However, the placement of the inflammatory response in AD neurodegenerative cascade is still debated, with conflicting ideas of innate

immune activation either being the trigger, a homeostatic response mechanism or a bystander phenomenon associated with the disease pathology [2].

Anti-inflammatory cytokines, such as Interleukin (IL) - 4, lead to the suppression of pro-inflammatory responses in macrophages, microglia, T cells, and astrocytes [3]. Anti-inflammatory cytokines are thought to enhance A $\beta$  degradation through phagocytosis and receptor-mediated uptake leading to the abrogation of A $\beta$  induced cell death in APP transgenic mice [4,5] and primary glia [6]. Down regulation of IL-4 receptors contributes to aging related cognitive impairment [7]. Consequently, IL-4 or minocycline treatment leads to restored synaptic activity in rats following intracerebroventricular infusion of A $\beta$  [8]. However, emerging evidence has also shown that activation of the innate immune system may constitute a beneficial defense

\* Correspondence: [tgolde@ufl.edu](mailto:tgolde@ufl.edu)

<sup>1</sup>Center for Translational Research in Neurodegenerative Disease, Department of Neuroscience, University of Florida, 1275 Center Drive, Gainesville, PO Box #100159, FL 32610, USA

Full list of author information is available at the end of the article

mechanism to clear A $\beta$  from the CNS [9]. Data from our lab [10-12] and others [13-17] have demonstrated that glial activation can effectively clear A $\beta$  plaques. It is generally thought that although a sustained inflammatory response is neurotoxic, activation of the innate immune system can indeed have a beneficial function by clearing debris and possibly promoting repair.

In an effort to further understand the role of neuroinflammation on A $\beta$  plaque pathology and specifically to test the role of anti-inflammatory cytokines on A $\beta$  pathology, we utilized recombinant adeno-associated virus serotype 1 (rAAV2/1) to overexpress murine IL-4 (mIL-4) in the hippocampus of Amyloid precursor protein (APP) transgenic mice with pre-existing amyloid plaques. Our results show that mIL-4 expression resulted in exacerbated A $\beta$  deposition in APP transgenic mice brains after 6 weeks of expression. Biochemical analysis of mIL-4 overexpressing mice brains and phagocytosis assays in primary murine glia suggests that mIL-4 expression leads to increased A $\beta$  levels possibly as a result of reduced glia phagocytosis.

## Results

To explore the role of anti-inflammatory cytokines in regulating A $\beta$  accumulation in the CNS, we have used recombinant adeno-associated virus serotype 1 (rAAV2/1) to express mIL-4 in the brains of APP transgenic TgCRND8 mice. Recombinant AAV2 plasmids were packaged in AAV serotype 1 capsid as described previously [10] and rAAV2/1 viruses expressing mIL-4 or EGFP under the control of the cytomegalovirus enhancer/chicken  $\beta$ -actin promoter were used for further experiments. Adult TgCRND8 mice were stereotaxically injected with AAV2/1 constructs ( $1 \times 10^{13}$  particles/ml) into the CA layer of the hippocampus at 4 months (after A $\beta$  plaque deposition has started) and were analyzed after 6 weeks ( $n = 6$  for rAAV1-mIL-4;  $n = 6$  for rAAV1-EGFP). Immunohistochemical analysis with anti-EGFP antibody shows that the viral transgene is predominantly expressed in the hippocampal CA neurons, neuronal projections in the cortex and thalamus, and some overlying cortical neurons following 6 week expression of AAV1-EGFP (Additional file 1: Figure S1, A-I). No detectable expression was noted in the mid-brain, olfactory bulb or cerebellum. In previous studies AAV2/1-EGFP expression had minimal effects on amyloid pathology or gliosis when compared to naïve uninjected mice [10,18,19]; so, AAV1-EGFP injected animals were used as the control cohort in this study. For adult injected mice, the brain was coronally dissected 1 mm anterior and posterior to the point of injection and used for subsequent analysis. We did not observe any significant changes in GFAP immunoreactive astrocytes (Figure 1, A-D) or Iba-1 reactive microglia (Figure 1, E-H) in the hippocampus of mIL-4 expressing mice compared to control mice. A careful

quantification of the histological staining (GFAP and Iba-1) in mouse hippocampus using "Positive Pixel Count" program (Aperio, CA) showed that though mIL-4 expressing mice had less microglial activation in and around the injection area there were no significant changes in either astrocyte or microglial levels overall (Figure 1, I). Immunoblotting analysis with hippocampal lysates also showed essentially unchanged astrogliosis profile in mIL-4 and control cohorts (Figure 1, J-K). Analysis of mRNA from injected mice hippocampus showed significantly increased levels of mIL-4 (3.13 times over control) and mIL-10 (2.4 times over control) (Figure 1, L). No significant change in levels of pro-inflammatory cytokines, TNF- $\alpha$  and IFN- $\gamma$ , or cd11b (data not shown) was seen. Furthermore, this was accompanied by an increase in Arginase (4 times over control) (Figure 1, L), suggesting an establishment of an alternative "M2a" microglial phenotype [1,20]. Increased levels of CD200R (4.2 times over control) was also noted, similar to previous observations [21].

Analysis of plaque burden showed that there was a 33.5% increase in amyloid plaques in the hippocampus of mIL-4 expressing mice compared to EGFP expressing mice (Figure 2, A-E). There was a concomitant increase in insoluble A $\beta$  levels by biochemical analysis - 41% increase in A $\beta$ 42 levels and 55% increase in A $\beta$ 40 levels in the SDS extractable A $\beta$  levels (Figure 2, F) respectively and 76% increase in A $\beta$ 42 levels and 62% increase in A $\beta$ 40 levels in the formic acid extractable A $\beta$  levels respectively (Figure 2, G). Interestingly, the number of Thioflavin S stained "cored" plaques in the hippocampus of mIL-4 expressing mice (15.2% increase) did not increase significantly compared to controls (Figure 3, A-C). We next investigated whether the increase in A $\beta$  was due to changes in APP expression, APP processing, ApoE levels or phagolysosomal dysfunction. Neither APP expression nor CTF $\alpha$  expression or CTF $\beta$  levels were altered in mIL-4 expressing TgCRND8 mice compared to controls (Figure 4, A-B). We additionally tested for the levels of endogenous mouse prion protein as the mutant human APP transgene is expressed from mouse prion promoter [22]. No significant change in prion protein levels was apparent between the mIL-4 expressing transgenic mice brains and control cohorts (Figure 4, C-D). Additionally, no change in mouse endogenous APP levels or CTF $\alpha$  levels were seen in 5 month old mIL-4 expressing wild type B6/C3H littermates of TgCRND8 mice injected in the cerebral ventricles on day P2 (Figure 4, E-F), suggesting that mIL-4 does not change either the holo-APP levels or APP processing or prion promoter expression in vivo. Though inflammatory signaling can modulate apoE levels through modulation of Erks [23], no significant change in ApoE levels were seen in mIL-4 injected compared to control transgenic APP mice (Additional file 2: Figure S2, A-B). Autophagolysosomal dysfunction may lead to increased accumulation

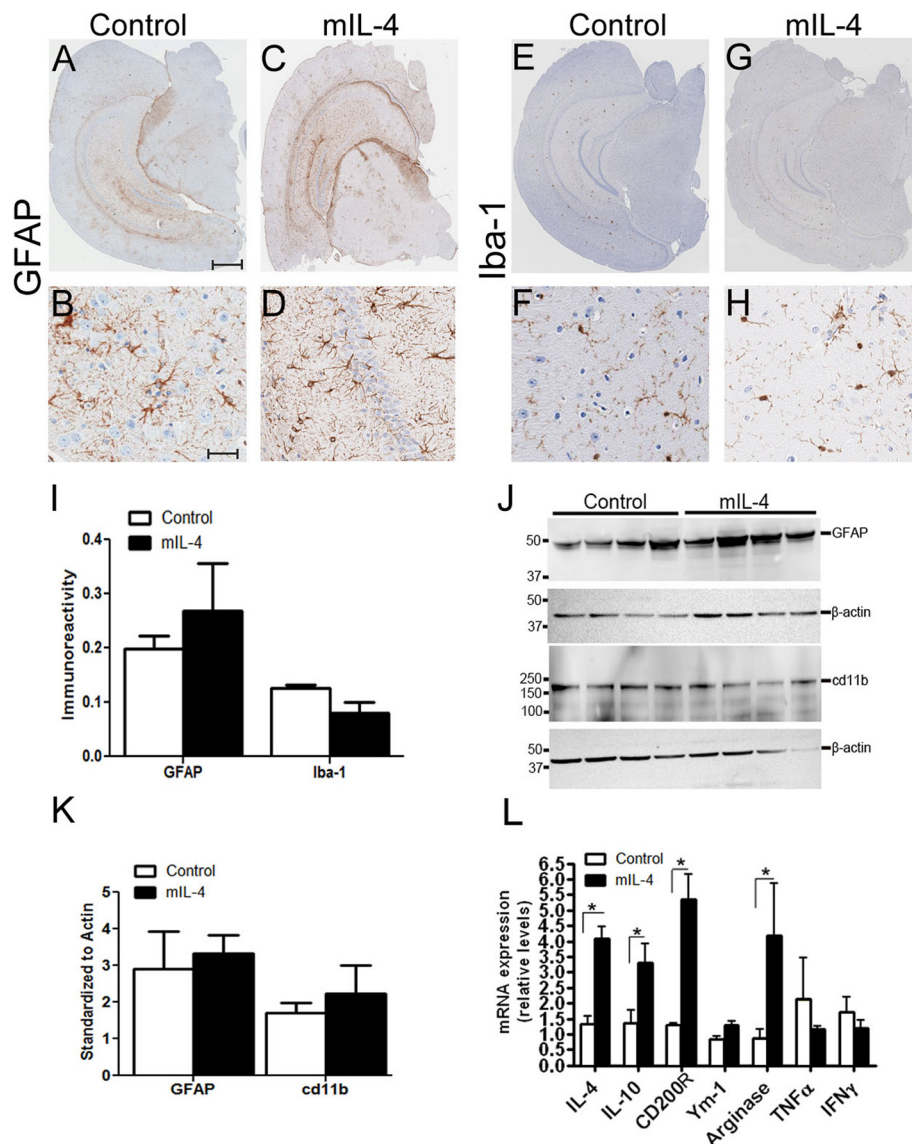


**Figure 1** AAV2/1 mediated expression of mIL-4 in TgCRND8 mice results in M2 phenotype. **A-D.** rAAV2/1-mIL-4 or rAAV2/1-EGFP (Control) was injected into the hippocampus of 4 month old TgCRND8 mice and analyzed after 6 weeks. Representative images of GFAP immunoreactivity in paraffin embedded whole brain sections (A, C) and higher magnification of the hippocampus (B, D) is shown. *Scale Bar*, 600  $\mu$ m (A, C) and 25  $\mu$ m (B, D). ( $n = 5-6$ /group). **E-H.** Representative images of Iba-1 immunoreactivity in paraffin embedded sections of 5.5 month old TgCRND8 mice injected with rAAV2/1 mIL-4 or rAAV2/1-EGFP (Control). Whole brain sections (E, G) and the corresponding hippocampus (F, H) are shown. *Scale Bar*, 600  $\mu$ m (E, G) and 25  $\mu$ m (F, H). ( $n = 5-6$ /group). **I.** Densitometric analysis of GFAP and Iba-1 immunostaining is shown. The hippocampal region was selected and Aperio "positive pixel count" program was used to measure percent positivity by averaging intensity of positive staining in the annotated region. ( $n = 4$ /group;  $p > 0.05$ ,  $t$  test). Data represents mean  $\pm$  sem. **J-K.** Representative immunoblot (J) and densitometric analysis of normalized levels of GFAP and cd11b (K) obtained from 5.5 month old TgCRND8 mice injected with rAAV2/1 mIL-4 or rAAV2/1-EGFP ( $n = 5$ /group;  $p > 0.05$ ,  $t$  test). Data represents mean  $\pm$  sem. **L.** Expression of glial activation markers and cytokines were determined in 5.5 month old mIL-4 expressing TgCRND8 mice compared to EGFP expressing age-matched controls using real time Q-PCR. Data, expressed as relative levels of mRNA expression, represents averaged fold change values obtained from mIL-4 expressing mice, relative to averaged values obtained from EGFP expressing mice. ( $n = 4$ /group;  $*p < 0.05$ ,  $t$  test). Data represents mean  $\pm$  sem.

of A $\beta$  [24]. Since anti-inflammatory cytokines, for example, IL-4 and IL-13, have been shown to inhibit autophagy [25], we tested whether changes in autophagic response may account for increased A $\beta$  accrual in mIL-4 expressing mice. No significant changes in the autophagic marker LC3-I

were seen in transgenic TgCRND8 mice injected with AAV2/1-mIL-4 (Additional file 3: Figure S3, A, D), though a nonsignificant lowering trend was observed in the non-transgenic cohort (Additional file 3: Figure S3, B, D). We were unable to detect LC3-II in the lysates, making it



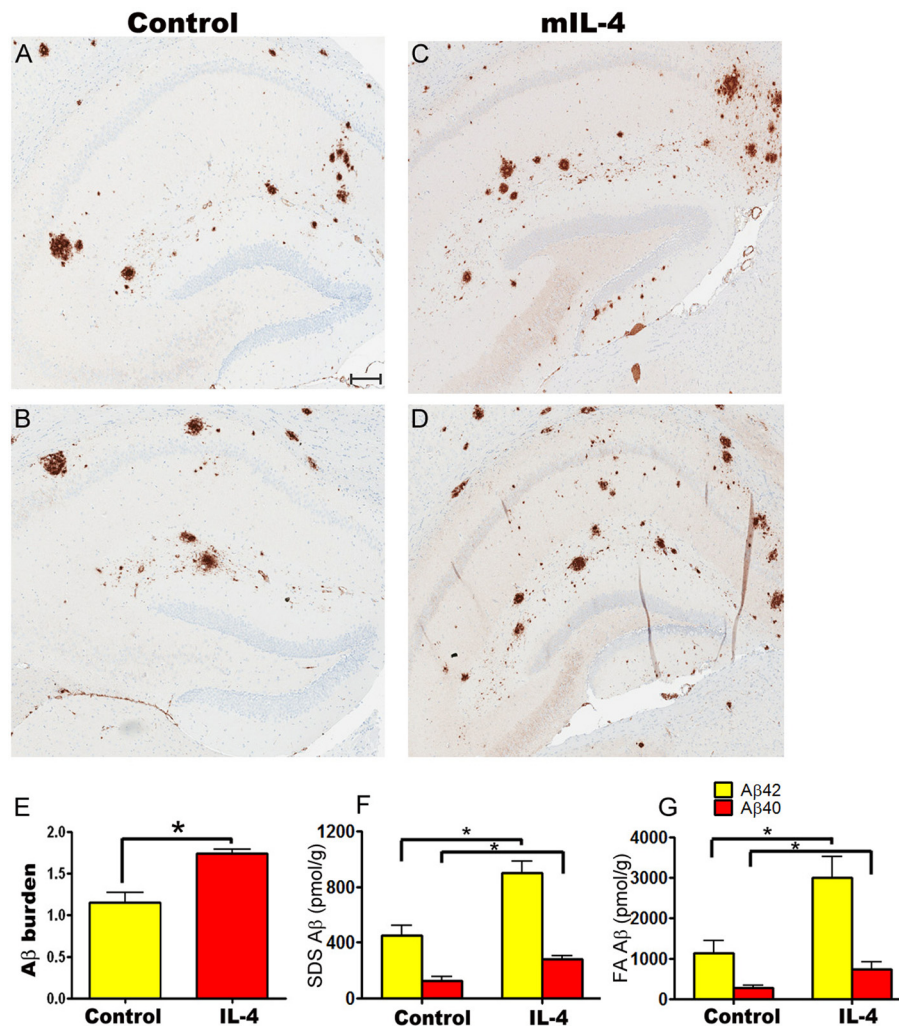


**Figure 2** Increased Aβ deposition in AAV1-mIL-4 expressing TgCRND8 mice. **A-D.** 4 month old TgCRND8 mice were stereotaxically injected in the hippocampus with either AAV1-mIL-4 (C, D) or AAV1-EGFP (A, B) and sacrificed after 6 weeks ( $n = 5-6$ /group). Representative brain sections stained with 33.1.1 antibody (pan Aβ 1–16) depict increased Aβ deposition in mIL-4 expressing mice (C, D) compared to controls (A-B) in the immediate vicinity of the injection site. Scale Bar, 150 μm. **E.** Aβ plaque burden analysis shows a significantly increased amyloid deposition in mIL-4 injected mice compared to control EGFP injected mice ( $n = 5$ /group). (\* $p < 0.05$ ,  $t$  test). Data represents mean ± sem. **F-G.** Biochemical analyses of Aβ42 and Aβ40 levels by ELISA show significantly increased SDS (F) and formic acid (G) extractable Aβ levels in mIL-4 injected mice compared to controls ( $n = 5$ /group). (\* $p < 0.05$ ,  $t$  test). Data represents mean ± sem.

difficult for us to infer effects of mIL-4 on autophagic flux in vivo. p62 (or sequestosome-1), which is a central player in autophagy was found to be decreased by 47% in mIL-4 expressing mice (Additional file 3: Figure S3, C-D).

A basic tenet of the amyloid cascade hypothesis is that Aβ accumulation triggers the onset and severity of neurodegenerative pathology, including tau hyperphosphorylation. Though occasional CP13 immunoreactive glial cells were visible in both mIL-4 and control mice, mIL-4 mice did not lead to appearance of phosphorylated CP13 immunoreactive tau (phospho Ser202/Thr205) in the hippocampal neurons in TgCRND8 mice, (Additional file 4: Figure S4, A-B). Immunoblotting also failed to show

any detectable levels of CP13 or MC6 (phospho Ser235) or PHF1 epitope (phospho Ser396/Ser404) in both cohorts (data not shown).

To further investigate the mechanism of mIL-4 induced Aβ accumulation, we treated primary wild type mouse neuroglial cultures with rAAV2/1-mIL-4 for 72–80 hours. Analysis of the conditioned media of these cells revealed increased mIL-4 protein ( $p < 0.01$ ,  $t$  test) but no increases in mIL-6 (data not shown) or mIFN-γ protein compared to control cultures (Figure 5, D). In addition, primary cultures transduced with mIL-4 showed increased levels of nuclear phosphorylated STAT6 compared to mIFN-γ or untreated cultures

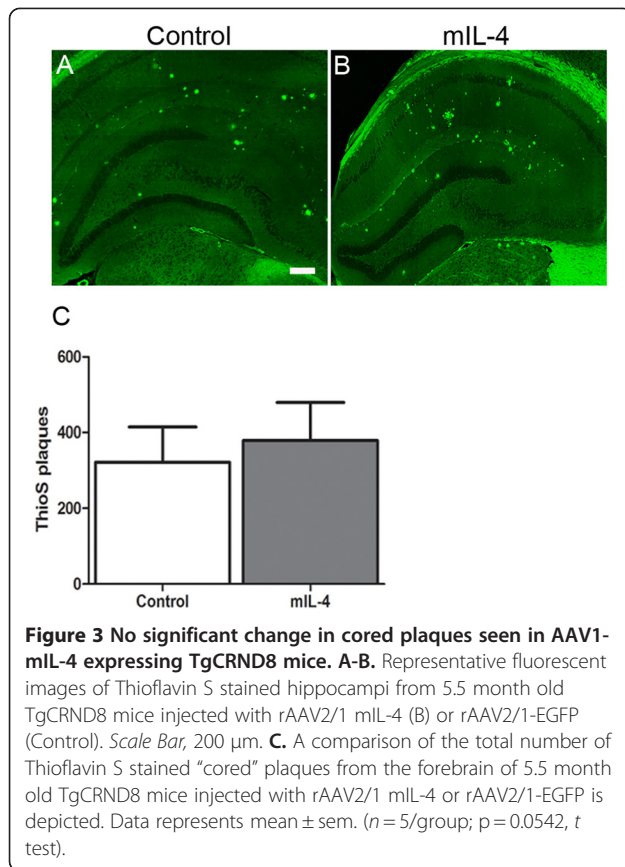
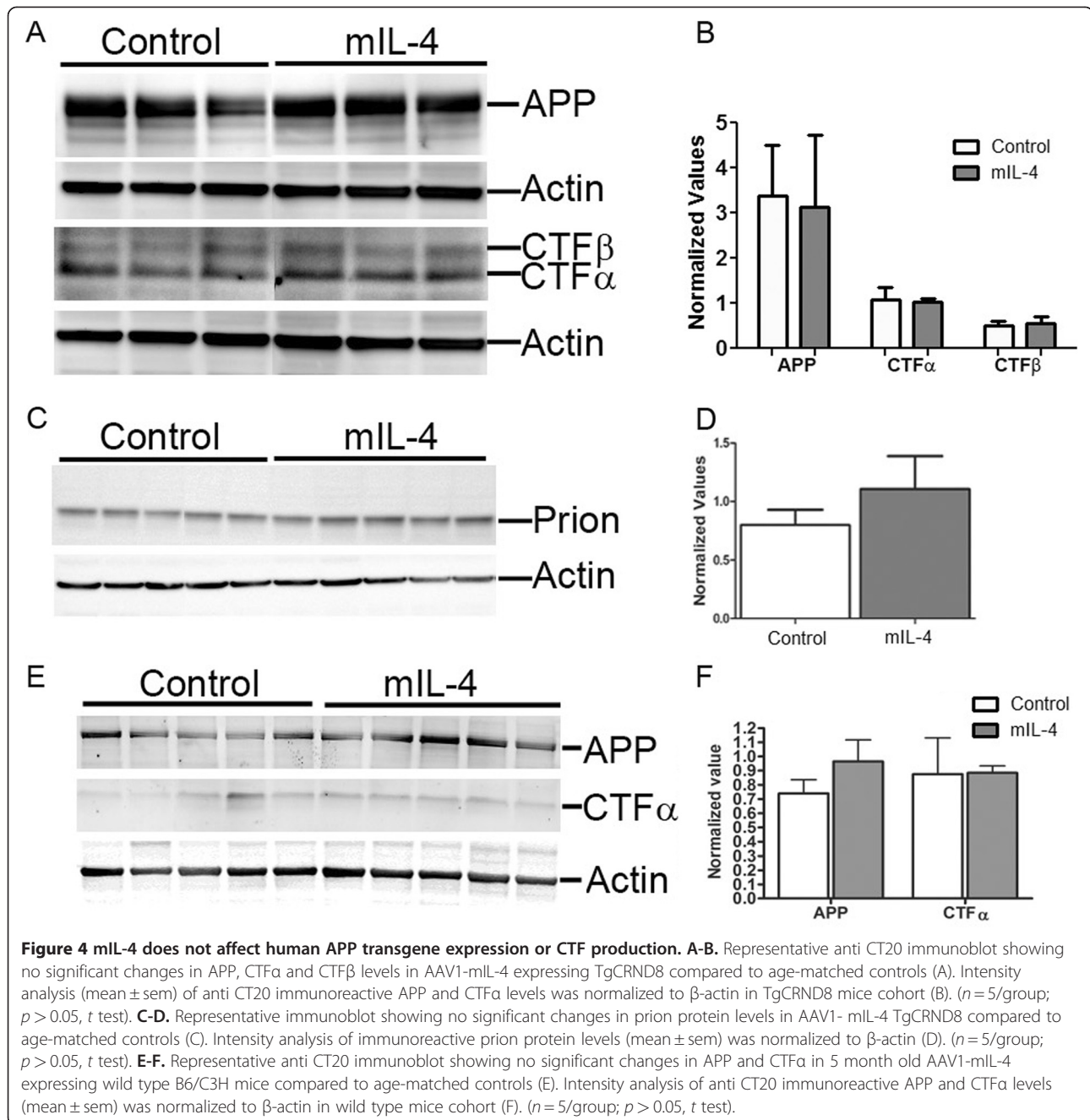


(Figure 5, A-C). Quantitative RT-PCR analysis confirmed increased mIL-4 ( $4.5e3$  x) levels as well as increased levels of cd11b (6 x), scavenger receptor A (3.3 x) and scavenger receptor B1 (15.6 x) (Figure 5, E). No significant changes in mouse APP, BACE1, or A $\beta$  degrading enzymes (IDE or Neprilysin) were seen (Figure 5, E). Since increased cd11b and scavenger receptors may result in altered phagocytic potential of mIL-4 expressing glia, we performed phagocytosis assays on mouse primary glia and astrocytes treated with medium alone or recombinant mIL-4. Since A $\beta$ 40 and A $\beta$ 42 can have different effects on phagocytosis, we used both to test out how mIL-4 affects astroglial phagocytosis. Primary mouse glia were treated with recombinant cytokines or vehicle for 10 hours, and fresh media added before incubation with fluorescent A $\beta$  for different times (Figure 6, Additional file 5: Figure S5– Additional file 6: Figure S6). These experiments were performed with cultures containing >95% CD45 and Cd11b immunopositive glia (Additional file 5: Figure S5, A-B). Initial microscopic examination showed a decrease in the levels of internalized A $\beta$ 40 in mIL-4 treated microglia following 15 min, 30 min or 60 min incubation with A $\beta$ 40-555 nm (Additional file 6: Figure S6, A-I). This was confirmed by flow cytometric analysis which showed a significant decrease in internalized fluorescent A $\beta$ 40 in mIL-4 treated

microglia at these three different timepoints (15 min: -19%; 30 min: -38%; 60 min: -19%) (Figure 6, A; Additional file 5: Figure S5, D-L). Since we have previously shown that mIL-6 treatment augments microglial A $\beta$  phagocytosis [10], we included this as an internal control for A $\beta$ 40 internalization in the flow cytometric assay (15 min: +29%; 30 min: +13%; 60 min: +41%) (Figure 6, A; Additional file 5: Figure S5, J-L). Immunoblotting of microglial cells following A $\beta$ 40 phagocytosis also showed that mIL-4 treated glia take up A $\beta$  less efficiently (Additional file 5: Figure S5, M-N). In order to test whether fibrillized A $\beta$ 42 (fA $\beta$ 42) has a different effect on glial phagocytosis, we performed phagocytosis assays using A $\beta$ 42 fibrils (Figure 6B). Flow analysis shows that neither mIL-6 (15 min: +25.7%; 30 min: +28%; 60 min: +8%) nor mIL-4 (15 min: +0.53%; 30 min: +8.1%; 60 min: +10.4%) significantly affects fA $\beta$ 42 internalization by microglia (Figure 6B). Since IL-4 can potentially activate astrocytic internalization of A $\beta$ , we performed phagocytosis with murine astrocyte cultures (Figure 6, C-D). Overall, neonatal astrocytes were very inefficient in internalizing A $\beta$ 40 as shown earlier [2,26]. Flow cytometric analysis shows that mIL-4 does not significantly alter astrocytic A $\beta$ 40 phagocytosis (15 min: +39.5%; 30 min: +50%; 60 min: +12.2%) (Figure 6, C) whereas mIL-6 increases astrocytic A $\beta$ 40 internalization significantly at all timepoints tested (15 min: +83.1%; 30 min: +58.3%; 60 min: +85.2%) (Figure 6, C). On the other hand, mIL-4 (15 min: -16.8%; 30 min: +3%) as well as mIL-6 (15 min: -48.4%; 30 min: -26%) has negligible effects on astrocytes phagocytosing fA $\beta$ 42 at the two earlier timepoints tested (Figure 6, D). Only at the last timepoint tested, i.e., following 60 min of incubation of fA $\beta$ 42, both mIL-4 (60 min: +44.4%;  $p < 0.05$ , 1 way Anova) and mIL-6 (60 min: +45%) enhances fA $\beta$ 42 uptake by primary astrocytes (Figure 6, D).

## Discussion

We have found that overexpression of mIL-4 in the hippocampus of plaque-depositing APP CRND8 mice increased A $\beta$  plaque pathology. We extensively investigated the likely factors that could be responsible for the effects of mIL-4 expression on increased A $\beta$  burden *in vivo*. APP, APP CTE, BACE, ApoE and A $\beta$  degrading enzyme levels did not appear to be altered. As IL-4 has been reported to inhibit autophagy [27], we investigated LC3I/II levels, but this was not informative, as we could not reliably detect LC3II. Levels of another key regulator of autophagy, p62, were decreased by mIL-4. As p62 has pleiotropic functions in addition to its role in autophagy [28] the significance of this finding is unclear. Furthermore if autophagic pathways were being inhibited, p62 would be expected to increase, not decrease. Given i) that these data indicating that mIL-4 does not appear to



be affecting APP processing and is not altering major A $\beta$  chaperones or degrading enzymes and ii) that we and others have previously linked proinflammatory activation of microglia to reduced plaque burdens and enhanced microglial scavenging of A $\beta$  [10,11,13,14,17,29,30], we hypothesize that mIL-4 increases A $\beta$  burden via reductions in glial scavenging of A $\beta$ . We explored this hypothesis through A $\beta$  internalization studies in primary

microglia and astrocytes cultures. These studies do show that mIL-4 abrogates soluble A $\beta$ 40 uptake by microglia without affecting aggregated fA $\beta$ 42 phagocytosis. Additionally, mIL-4 does not affect the uptake of soluble or aggregated A $\beta$  by astrocytes, though on longer incubation, there was an increasing trend in A $\beta$  ingestion by the astrocytes. Given the low number of astrocytes internalizing A $\beta$  and the fact that astrocyte cultures may



contain ~10-20% microglia, it is difficult to conclude whether astrocytes by themselves have a critical role in A $\beta$  phagocytosis.

Microglia can scavenge A $\beta$  via receptor-mediated phagocytosis as well as macropinocytosis [26]. In vivo imaging techniques have demonstrated that microglia

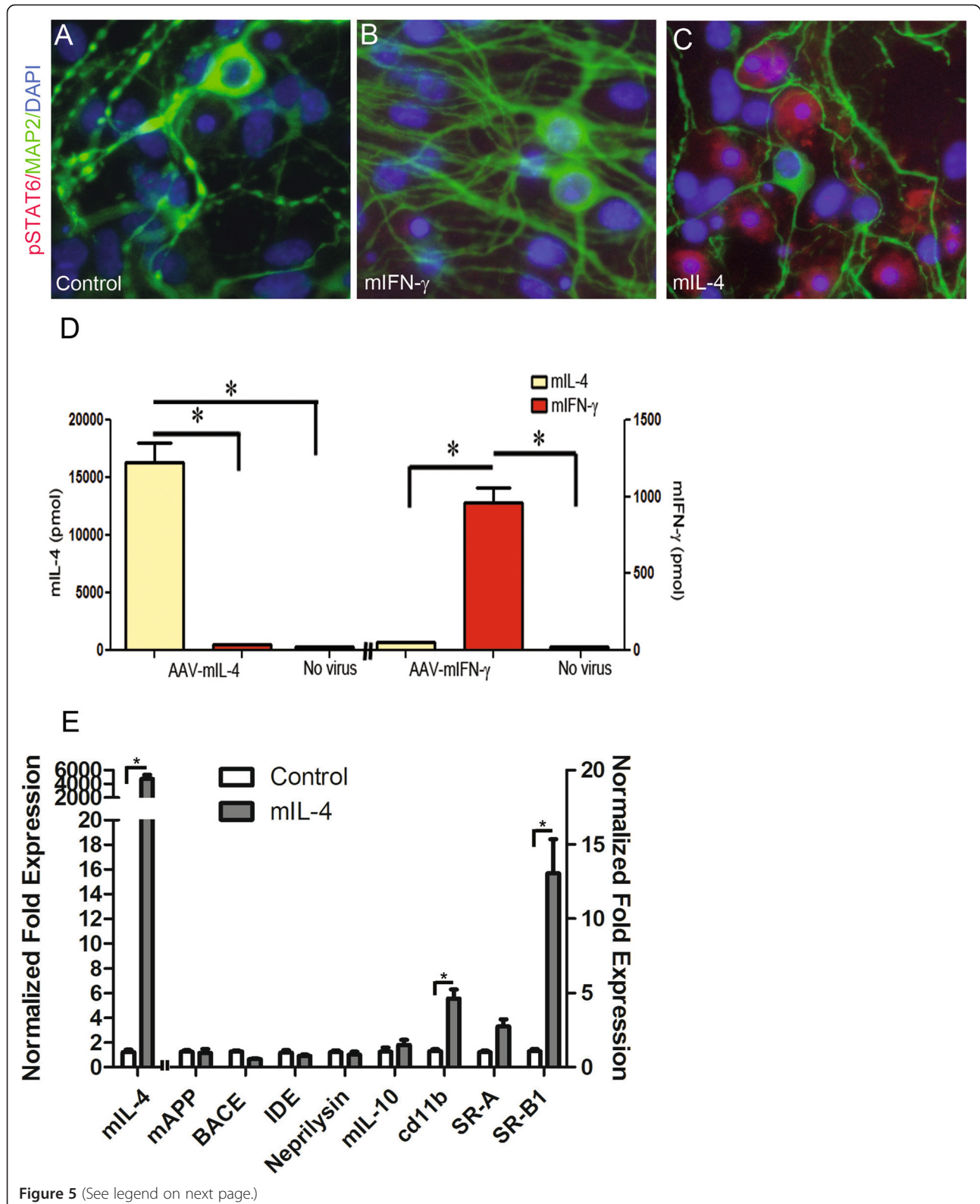


Figure 5 (See legend on next page.)

(See figure on previous page.)

**Figure 5 Characterization of rAAV2/1-mIL-4 treated primary wild type mouse neuroglial culture. A-D.** rAAV2/1-mIL-4 or rAAV2/1-mIFN- $\gamma$  ( $2 \times 10^8$  viral genomes) was used to transduce primary mouse neuroglial cultures for 60 hrs in chamber slides. Upregulation of phosphorylated STAT6 (568 nm; red fluorescence) could be seen in mIL-4 expressing cultures (C) but not in mIFN- $\gamma$  expressing cultures (B) or untreated culture containing no viruses (A). MAP2 (488 nm; green) and DAPI (350 nm, blue) were used to depict neuronal processes and nucleus respectively. mIL-4 and mIFN- $\gamma$  expression in these cultures was verified by ELISA from media collected from respective cultures (D). Magnification, 400x. (\* $p < 0.05$ ,  $t$  test). **E.** Expression of mouse endogenous APP, BACE1, IDE and neprilysin levels are unchanged in rAAV2/1-mIL-4 expressing primary mixed neuroglial cultures compared to untreated control cultures using real time Q-PCR. mIL-4 expression augments scavenger receptors and cd11b levels. Data, expressed as relative levels of mRNA expression, represents averaged fold change values obtained from mIL-4 expressing mice, relative to averaged values obtained from EGFP expressing mice. Data for mIL-4 RNA is plotted on the left x-axis while the rest of the data are plotted on the right x-axis. Data is representative of two independent experiments ( $t$  test, \* $p < 0.05$ ). Data represents mean  $\pm$  sem.

can home onto newly appearing plaques and internalize A $\beta$  [31]. Microglial interaction with A $\beta$  occurs through several cell surface receptors, for example, SR-A, SR-B, integrins and Toll-like receptors [15,32-34]. Previous studies have noted that inflammatory cytokines decrease scavenger receptors levels in microglial cell lines and

inhibit A $\beta$  uptake [35]. We find that mIL-4 expression leads to increased SRs in mixed neuroglial cultures, but this appears to be linked to modest inhibitory effects on soluble, but not aggregated, A $\beta$  uptake by microglia. Therefore, it is possible that in the absence of inflammatory mediators, these cells are not competent for A $\beta$

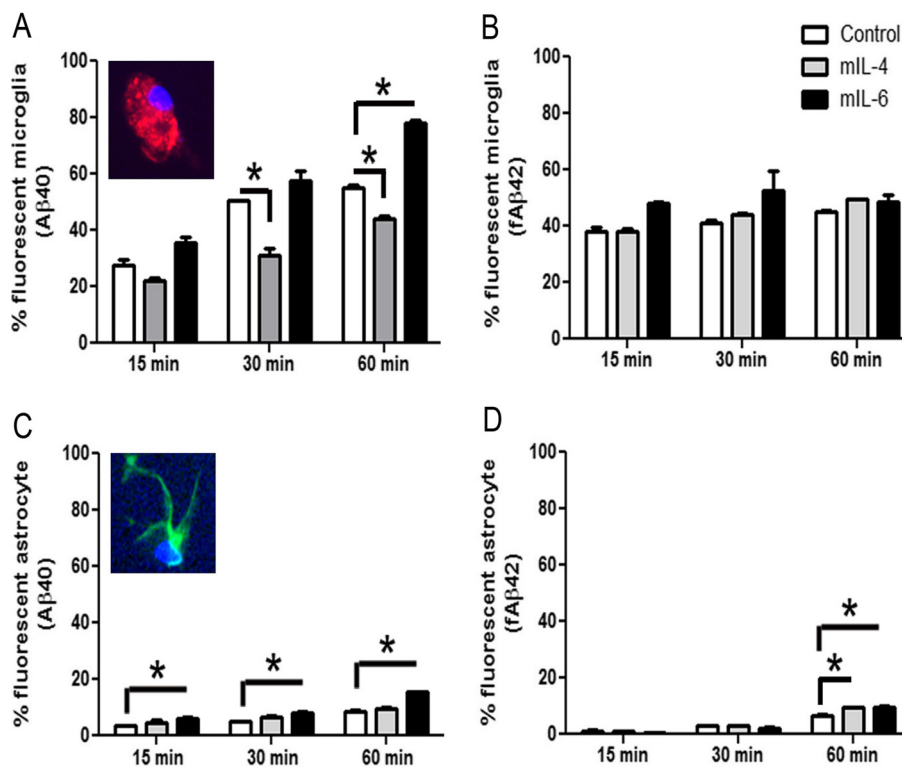


**Figure 6 Differential effect of cytokines on A $\beta$ 40 and fA $\beta$ 42 uptake by primary mouse glia and astrocytes. A-B.** mIL-4 treatment decreases microglial uptake of A $\beta$ 40 (A) but does not affect fA $\beta$ 42 uptake (B). mIL-6 increased microglial A $\beta$ 40 uptake (A) but does not significantly alter fA $\beta$ 42 uptake (B). Primary mouse glia were treated with recombinant cytokines for 10 hrs and incubated with A $\beta$ 40-Hilyte555 or A $\beta$ 42-Hilyte555 for 15 min, 30 min and 60 min. Trypsinized cells were counted using Accuri6 flow cytometer. Unstained cells and labeled additives were excluded by gating to yield the percentage of fluorescent cells in the mix. Inset depicts cd11b/DAPI stained glia (A) Results are representative of three independent experiments. (\* $p < 0.05$ , One way Anova with Tukey's post test). Data represents mean  $\pm$  sem. **C-D.** mIL-4 treatment does not affect astrocytic uptake of A $\beta$ 40 (C) but increases fA $\beta$ 42 uptake after 60 min incubation (D). mIL-6 consistently increases astrocytic A $\beta$ 40 uptake (C) and only enhances fA $\beta$ 42 uptake after 60 min incubation (D). Primary mouse astrocytes were treated with recombinant cytokines for 10 hrs and incubated in A $\beta$ 40-Hilyte555 or A $\beta$ 42-Hilyte555 for 15 min, 30 min and 60 min. Trypsinized cells were counted using Accuri6 flow cytometer. Unstained cells and labeled additives were excluded by gating to yield the percentage of fluorescent cells. Inset depicts GFAP/DAPI labeled astrocyte (C). Results are representative of two independent experiments. (\* $p < 0.05$ , One way Anova with Tukey's post test). Data represents mean  $\pm$  sem.



internalization and degradation, even if they express the receptors [36,37]. Indeed, microglia were found to require stimulation with cytokines or opsonins for internalizing and degrading A $\beta$  efficiently in amyloid vaccination paradigms [38]. Microglial populations from human AD brains display an IL-4/IL-13 induced alternate activation profile [39] as well as increased IL-1 $\beta$ , suggesting that an imbalance between the inflammatory “classical” and anti-inflammatory alternate activation profiles may result in a dysfunctional glial response and “failed” phagocytosis. Although speculative, these studies may have relevance to human therapy. Many studies show an association of nonsteroidal anti-inflammatory drugs (NSAIDs) use with reduction of dementia risk [40]. However, in the Adult Changes in Thought (ACT) study, there was an increased incidence of all-cause dementia and AD dementia in individuals with heavy non-selective NSAID use, and this was associated with an increase in neuritic plaques at autopsy [41]. Our data could provide an explanation for this association.

It is generally accepted that an altered innate immune response is an inherent feature of AD and most, if not all, degenerative, CNS proteinopathies [42]. Though a large body of literature on this subject refers to this altered immune response as “pathogenic” or “harmful”, in many cases this relationship is assumed and has not been formally proven. Increased pro-inflammatory cytokines levels (TNF $\alpha$ , Interleukin-6, Interleukin-1 $\beta$ ), combined with decreased levels of anti-inflammatory cytokines (Interleukin-10), have been correlated with cognitive deficits suggesting that early inflammatory changes may be detrimental [43]. Furthermore pro-inflammatory stimuli have been linked to overt neuronal degeneration [44]. Although pro-inflammatory factors may have a detrimental role on neuronal function, priming of CNS microglia and possibly astrocytes by accumulating A $\beta$ , may be an essential innate host response that triggers glial phagocytosis activity and clears A $\beta$  deposits. Indeed, we and others have previously shown that activation of the innate immune signaling pathways can attenuate A $\beta$  accumulation in APP transgenic mice and alter the disease process [10-14,17,29,30].

mIL-4 has been shown to enhance A $\beta$  phagocytosis in primary rodent glial cultures in vitro [45,46]. Based largely on such evidence, promotion of a glial M2 phenotype has been proposed to be beneficial in preclinical AD models and this concept was directly supported by one recent study, using a similar AAV mediated IL-4 expression paradigm as used in this present study [4]. In this study IL-4 induced a Th2 like glial phenotype, but in contrast to our results, Kiyota et al, showed that IL-4 expression in the hippocampus led to mitigation of A $\beta$  pathology and improved behavior in APP/PS1 mice [4]. Inherent differences in transgenic mice as well as

experimental paradigms may underlie the disparate observations. It is possible that presenilins may regulate cytokine secretion [47], and mutant PS1 especially may confer altered sensitivity to immune challenges in the resident glial cells [48]. Additionally, the two studies were distinct with respect to initiation of treatment. Kiyota and colleagues performed a primary prevention study in which IL-4 expression was initiated in the pre-deposition phase, whereas IL-4 expression in our studies was initiated in mice with modest levels pre-existing plaques. In any case, additional studies of both IL-4 and other anti-inflammatory factors will be required to address this discrepancy and the generalizability of this finding.

### Conclusion

In summary, we demonstrate that focal overexpression of mIL-4 in APP transgenic mouse brains leads to exacerbated A $\beta$  plaque pathology. As these results are opposite of effects observed with proinflammatory cytokines, we would suggest that the underlying mechanism appears to be at least in part a failure of glia to successfully clear A $\beta$ . Our data points to the complex relationship between microglial phenotype and the final functional outcome, necessitating a more cautious and thorough examination of potential anti-inflammatory therapies for AD.

### Methods

**Mice.** All animal husbandry procedures performed were approved by the Institutional Animal Care and Use Committee.

**AAV1 preparation and injection.** AAV1 viruses expressing mIL-4 or EGFP, under the control of the cytomegalovirus enhancer/chicken  $\beta$  actin promoter were generated as described previously [19]. For stereotaxic injections, TgCRND8 mice (n = 6/group) were anesthetized with 1.5% isoflurane in 1% oxygen and secured into a Kopf apparatus (Model 900 Small Animal Stereotaxic Instrument, David Kopf Instruments). The coordinates for injection were -1.7 caudal, -1.6 lateral and -1.2 ventral from the bregma. A UMP2 Microsyringe Injector and Micro4 Controller (World Precision Instruments, USA) was used to inject 2  $\mu$ l ( $10^{10}$  viral genomes) of virus at a constant rate over a 10 minute period. After allowing an additional 10 minutes, the needle was raised and the scalp incision was closed aseptically. Nontransgenic mice used in the study were injected with rAAV2/1-mIL-4 on day P2 into the cerebral ventricles and aged till 5 months of age.

**Quantitative real-time PCR.** Total RNA from mice hippocampus or primary wild type mouse neuroglial cultures was isolated using the RNeasy kit (Ambion) and reverse transcribed using Superscript III (Invitrogen).

The Q-PCR (initial denaturation cycle of 95 °C /10 min, followed by 40 amplification cycles of 95 °C /15 s and 60 °C/ 1 min) was performed with ABI Prism 7900 Real Time PCR System (Applied Biosystems) using SYBR Green to detect the amplification products. Relative quantification of mRNA expression was calculated by the  $\Delta C_T$  method described by the manufacturer (ABI Prism 7700 Sequence Detection System, User Bulletin #2) after adjusting the levels to the corresponding internal actin control for each sample. Primers and probes were designed following Roche Universal Probe Library sequences (Hoffmann-La Roche, Germany).

**Preparation of brain homogenate for immunoblotting and A $\beta$  ELISA assay.** Brain were coronally dissected 1 mm anterior and posterior to the point of injection and used for subsequent analysis. Thus, the samples for immunoblotting were obtained by dissecting the hippocampus and overlying cortex and thalamus of injected brains. Protein samples (RIPA soluble or 2% SDS soluble) separated on Bis-Tris 12% XT gels (Bio-Rad, USA) were probed with the antibody CT20 (anti-APP C-terminal 20 amino acid; T. E. Golde; 1:1000); 82E1 (IBL, 1:500), Prion (Abcam; 1:1000); LC3 (MBL; 1:500; Cell Signaling, 1:250; Novus, 1:500); p62 (Cell Signaling, 1:250), CP13 (P. Davies; 1:500) and anti  $\beta$ -actin (Sigma, 1:1000). Relative band intensity was quantified using ImageJ software (NIH).

A $\beta$  levels were determined biochemically using human A $\beta$  end-specific sandwich ELISA as previously described [19] on samples sequentially extracted with RIPA buffer, 2% SDS and 70% Formic Acid. All ELISA results were analyzed using SoftMax Pro software (Molecular Device).

**Immunohistochemical imaging and image processing.** Brains were coronally dissected at the point of injection for analysis. Immunohistochemical staining was done using pan A $\beta$  antibody 33.1.1 (1:1500, T. Golde), 82E1 (1:500, IBL), Iba-1 (1:1000; Wako), GFAP (1:500; Chemicon), pSTAT6 (1:500, Cell Signaling) and MAP2 (1:1000; Chemicon). 1% Thioflavin S (Sigma) staining was done on paraffin embedded brain sections using established protocols.

Immunohistochemically and fluorescent stained sections were captured using the Aperio Scanscope XT or FL image scanner and analyzed using either Aperio positive pixel count or ImageJ program. Brightness and contrast alterations were applied identically on captured images using Adobe Photoshop CS3.

**Quantification of A $\beta$  deposition and gliosis.** Paraformaldehyde fixed paraffin embedded brain tissue sections were immunostained with 33.1.1 antibody. A $\beta$  plaque burden and intensity of astrogliosis staining was calculated using the Positive Pixel Count program (Aperio). At least three sections per sample, 30  $\mu$ m apart, were

averaged by a blinded observer to calculate plaque burden. For Thioflavin S quantitation, one section per sample was used by a blinded observer to manually count the plaques using Adobe Photoshop CS5.

**Primary murine culture and microglia/astrocyte phagocytosis assay.** Primary microglia, astrocytes or neuronal cultures (mixed with astrocytes) were obtained from cerebral cortices of wild type neonate mice as described previously [38]. Glial and astrocytic cultures typically were >90% cd11b (cd11b-APC; 1:200, BD Biosciences) or GFAP (Sigma, 1:500) immunopositive respectively. For phagocytosis assays, microglia or astrocytes, pre-treated with mIL-4 (R&D Systems, USA; 5 ng/ml for 10 hours) or mIL-6 (R&D Systems, USA; 10 ng/ml for 10 hours) were incubated with 0.5  $\mu$ M Hilyte555-A $\beta$ 40 (Anaspec, USA) or fibrillar Hilyte555-A $\beta$ 42 (Anaspec, USA). Recombinant fluorescent A $\beta$  was resuspended in DMSO to 1 mg/ml and diluted in DMEM medium to 0.5  $\mu$ M before addition to cells. Hilyte555-A $\beta$ 42 was fibrillized at 37<sup>o</sup> C for 6 hours in PBS. Cells were analyzed at three timepoints following addition of A $\beta$  to the culture at 37<sup>o</sup> C: 15 min, 30 min and 1 hr. Cells were washed, gently trypsinised to remove cell surface associated fluorescent entities, fixed in paraformaldehyde and mounted in DAPI containing medium for visualization. Fluorescence intensity of individual cells from at least 5 or more fields of views per sample were calculated from Image J and averaged. For FACS analysis, following washes, cells were collected by trypsinization and resuspended in FACS buffer containing BSA and scanned. Scans were collected using Accuri6 and analyzed with FCS Express 4 Flow Research (BD Biosciences). Neuronal cultures were transduced with AAV (mIL-4 or mIFN- $\gamma$ ; 10<sup>8</sup> viral genomes) on day 7 for 60 hours and fixed with paraformaldehyde for subsequent immunocytometry. Cytokine ELISA was performed using BD Bioscience OptiEIA reagents.

#### Statistical analysis

One-way Anova (with Tukey's post-hoc test) or two-tailed Student's t test was used for statistical comparison (SigmaStat 3.0 version). Graphical analyses were done using Prism 4 (GraphPad Software) and final images created using Photoshop CS2 (Adobe).

#### Additional files

**Additional file 1: Figure S1.** rAAV2/1-EGFP expression in TgCRND8 mice hippocampus. **A-I.** Representative image obtained from mice stereotactically injected with AAV2/1-EGFP in the hippocampus. 4 month old TgCRND8 were injected into the hippocampus and analyzed after 6 weeks. Representative images of EGFP immunoreactivity on paraffin embedded whole brain section (A), cortex (B), hippocampal CA neurons (C-E), midbrain, (F), cerebellum (G), thalamus (H) and olfactory bulb (I) are shown. Representative hippocampus from uninjected mice is shown as

control (A, inset). I-V, cortex layers I to V; CC, corpus callosum; Sp, Septum; Th, thalamus. *Scale Bar*, 600  $\mu$ m (A) and 85  $\mu$ m (B-I).

**Additional file 2: Figure S2.** mIL-4 expression does not alter ApoE levels. **A-B.** No significant change in ApoE levels was seen in the hippocampus of mIL-4 expressing 5.5 month old transgenic CRND8 mice or age-matched control cohorts (A). Intensity analysis of ApoE levels was normalized to  $\beta$ -actin (B). ( $n = 5-6$ /group;  $t$  test,  $p > 0.05$ ).

**Additional file 3: Figure S3.** mIL-4 expression does not alter levels of the autophagic marker LC3 but decreases p62 protein levels. **A-B.** No significant change in the autophagic marker (microtubule-associated protein light chain 3, LC3) was seen in mIL-4 expressing 5.5 month old transgenic CRND8 mice (TG, A) or nontransgenic 5 month old nontransgenic cohorts (NTG, B). **C.** p62 protein levels decrease in mIL-4 expressing 5.5 month old transgenic CRND8 mice (TG). **D.** Intensity analysis of anti LC3 and p62 immunoreactive band after normalization to  $\beta$ -actin immunoreactivity. ( $n = 4-6$ /group). (\* $p < 0.05$ ;  $t$  test).

**Additional file 4: Figure S4.** mIL-4 expression does not alter levels of phosphorylated tau. No significant change in phosphorylated tau (using CP13 antibody) was seen in the hippocampus of mIL-4 expressing 5.5 month old transgenic CRND8 mice (**B**) or age-matched control cohorts (**A**). Occasional CP13 immunoreactivity was seen in glial cells in the pyramidal layer of the hippocampus (inset). *Scale Bar*, 150  $\mu$ m (A, B) and 25  $\mu$ m (inset). ( $n = 6$ /group).

**Additional file 5: Figure S5.** Analysis of primary mouse microglial culture following A $\beta$ 40 phagocytosis. **A-B.** Representative flow cytometric analysis of unstained (A) and CD45-FITC stained mouse microglia (B). Glial populations used for subsequent phagocytosis experiments were  $>95\%$  positive for both CD45 and cd11b. Inset in A depicts a representative unstained primary mouse glial culture. Magnification, 200x. **C-L.** Primary mouse glia were stimulated with medium alone (Control; D-F) or recombinant mIL-4 (5 ng/ml; G-I) or mIL-6 (10 ng/ml; J-L). After 10 hrs of stimulation, cells were incubated with fluorescent A $\beta$ 40 for 15 min (D, G, J), 30 min (E, H, K) or 60 min (F, I, L). Cells were trypsinized for the analysis of internalized fluorescent A $\beta$ 40 (D-L) by FACS. Unstained cells and additives have been gated for exclusion (C). Representative data from three independent experiments have been shown. Quantified data has been plotted in Figure 6A. **M-N.** Immunoblot analysis to detect presence of A $\beta$  in primary glial cells at different timepoints following A $\beta$ 40 phagocytosis in the presence or absence of mIL-4 (M). Intensity analysis of 82E1 immunoreactive A $\beta$  monomer after normalization to  $\beta$ -actin immunoreactivity has been shown (N). Representative data from two independent experiments have been shown.

**Additional file 6: Figure S6.** Microscopic analysis of A $\beta$ 40 phagocytosis by mIL-4 treated mouse primary glia. Primary mouse glia were treated with 5 ng/ml mIL-4 for 10 hrs and incubated with fluorescent A $\beta$ 40 for 0 min (A-B), 15 min (C-D), 30 min (E-F) or 60 min (G-H). Following gentle trypsinization, cells were fixed, stained with the nuclear stain DAPI and visualized. Inset (C) depicts mIL-6 treated glia after 15 min incubation with A $\beta$ 40. Quantitation of average fluorescent count is depicted (I). Magnification, 400x. (\* $p < 0.05$ ;  $t$  test).

#### Abbreviations

AAV: Adeno-associated virus; ACT: Adult Changes in Thought; AD: Alzheimer's disease; A $\beta$ : Amyloid  $\beta$ ; APP: Amyloid  $\beta$  precursor protein; ApoE: Apolipoprotein e4; BACE:  $\beta$ -site APP cleaving enzyme; CTF: C-terminal fragment; EGFP: Enhanced green fluorescent protein; Erk: Extracellular signal-regulated kinases; FACS: Fluorescence activated cell sorting; GFAP: Glial fibrillary acidic protein; IL-4: Interleukin-4; IFN- $\gamma$ : Interferon- $\gamma$ ; IACUC: Institutional animal care and use committee; Iba-1: Ionized calcium binding adaptor protein 1; LC3: Microtubule-associated protein light chain 3; NSAIDs: Nonsteroidal anti-inflammatory drugs; SR: Scavenger receptor; STAT: Signal Transducer and Activator of Transcription; TNF $\alpha$ : Tumor necrosis factor  $\alpha$ .

#### Competing interests

The authors declare no competing interests.

#### Authors' contributions

PC conducted the experiments and wrote the manuscript; LT performed immunostaining, primary mouse neuroglial culture, phagocytosis assays and flow cytometry; AB performed mouse brain Q-PCR and amyloid burden analysis; CC-D prepared recombinant AAV and Q-PCR of neuroglial culture; PD provided helpful discussion; TEG coordinated the research, supervised the project and assisted in manuscript preparation. All authors have read and approved the final manuscript.

#### Acknowledgements

This work was supported by Mayo Clinic (TEG), National Institutes of Health/National Institute on Aging Grants (RO1AG18454, RO1AG29886, P01AG25531; TEG) and American Health Assistance Foundation Grant A2009061 (PD).

#### Author details

<sup>1</sup>Center for Translational Research in Neurodegenerative Disease, Department of Neuroscience, University of Florida, 1275 Center Drive, Gainesville, PO Box #100159, FL 32610, USA. <sup>2</sup>Department of Neuroscience, Mayo Clinic College of Medicine, 4500 San Pablo Rd S, Jacksonville, FL 32224, USA.

Received: 15 February 2012 Accepted: 22 July 2012

Published: 29 July 2012

#### References

1. Cameron B, Landreth GE: Inflammation, microglia, and Alzheimer's disease. *Neurobiol Dis* 2010, **37**:503–509.
2. Wyss-Coray T, Loike JD, Brionne TC, Lu E, Anankov R, Yan F, Silverstein SC, Husemann J: Adult mouse astrocytes degrade amyloid-beta in vitro and in situ. *Nat Med* 2003, **9**:453–457.
3. Brown MA, Hural J: Functions of IL-4 and control of its expression. *Crit Rev Immunol* 1997, **17**:1–32.
4. Kiyota T, Okuyama S, Swan RJ, Jacobsen MT, Gendelman HE, Ikezu T: CNS expression of anti-inflammatory cytokine interleukin-4 attenuates Alzheimer's disease-like pathogenesis in APP + PS1 bigenic mice. *FASEB J* 2010, **24**:3093–3102.
5. Butovsky O, Koronyo-Hamaoui M, Kunis G, Ophir E, Landa G, Cohen H, Schwartz M: Glatiramer acetate fights against Alzheimer's disease by inducing dendritic-like microglia expressing insulin-like growth factor 1. *Proc Natl Acad Sci U S A* 2006, **103**:11784–11789.
6. Soria JA, Arroyo DS, Gaviglio EA, Rodriguez-Galan MC, Wang JM, Iribarren P: Interleukin 4 induces the apoptosis of mouse microglial cells by a caspase-dependent mechanism. *Neurobiol Dis* 2011, **43**:616–624.
7. Nolan Y, Maher FO, Martin DS, Clarke RM, Brady MT, Bolton AE, Mills KH, Lynch MA: Role of interleukin-4 in regulation of age-related inflammatory changes in the hippocampus. *J Biol Chem* 2005, **280**:9354–9362.
8. Lyons A, Griffin RJ, Costelloe CE, Clarke RM, Lynch MA: IL-4 attenuates the neuroinflammation induced by amyloid-beta in vivo and in vitro. *J Neurochem* 2007, **101**:771–781.
9. Rivest S: Regulation of innate immune responses in the brain. *Nat Rev Immunol* 2009, **9**:429–439.
10. Chakrabarty P, Jansen-West K, Beccard A, Ceballos-Diaz C, Levites Y, Verbeeck C, Zubair AC, Dickson D, Golde TE, Das P: Massive gliosis induced by interleukin-6 suppresses A $\beta$  deposition in vivo: evidence against inflammation as a driving force for amyloid deposition. *FASEB J* 2009, **24**:548–559.
11. Chakrabarty P, Ceballos-Diaz C, Beccard A, Janus C, Dickson D, Golde TE, Das P: IFN-gamma promotes complement expression and attenuates amyloid plaque deposition in amyloid beta precursor protein transgenic mice. *J Immunol* 2010, **184**:5333–5343.
12. Chakrabarty P, Herring A, Ceballos-Diaz C, Das P, Golde TE: Hippocampal expression of murine TNF $\alpha$  results in attenuation of amyloid deposition in vivo. *Mol Neurodegener* 2011, **6**:16.
13. El Khoury J, Toft M, Hickman SE, Means TK, Terada K, Geula C, Luster AD: Ccr2 deficiency impairs microglial accumulation and accelerates progression of Alzheimer-like disease. *Nat Med* 2007, **13**:432–438.
14. Shaftel SS, Kyrkanides S, Olschowka JA, Miller JN, Johnson RE, O'Banion MK: Sustained hippocampal IL-1 beta overexpression mediates chronic neuroinflammation and ameliorates Alzheimer plaque pathology. *J Clin Invest* 2007, **117**:1595–1604.
15. Richard KL, Filali M, Prefontaine P, Rivest S: Toll-like receptor 2 acts as a natural innate immune receptor to clear amyloid beta 1–42 and delay

- the cognitive decline in a mouse model of Alzheimer's disease. *J Neurosci* 2008, **28**:5784–5793.
16. Town T, Laouar Y, Pittenger C, Mori T, Szekely CA, Tan J, Duman RS, Flavell RA: **Blocking TGF-beta-Smad2/3 innate immune signaling mitigates Alzheimer-like pathology.** *Nat Med* 2008, **14**:681–687.
  17. Boissonneault V, Filali M, Lessard M, Relton J, Wong G, Rivest S: **Powerful beneficial effects of macrophage colony-stimulating factor on beta-amyloid deposition and cognitive impairment in Alzheimer's disease.** *Brain* 2009, **132**:1078–1092.
  18. Levites Y, Das P, Price RW, Rochette MJ, Kostura LA, McGowan EM, Murphy MP, Golde TE: **Anti-Abeta42- and anti-Abeta40-specific mAbs attenuate amyloid deposition in an Alzheimer disease mouse model.** *J Clin Invest* 2006, **116**:193–201.
  19. Kim J, Miller VM, Levites Y, West KJ, Zwizinski CW, Moore BD, Troendle FJ, Bann M, Verbeeck C, Price RW, *et al*: **BRI2 (ITM2b) inhibits Abeta deposition in vivo.** *J Neurosci* 2008, **28**:6030–6036.
  20. Mantovani A, Bonecchi R, Locati M: **Tuning inflammation and immunity by chemokine sequestration: decoys and more.** *Nat Rev Immunol* 2006, **6**:907–918.
  21. Lyons A, Downer EJ, Crotty S, Nolan YM, Mills KH, Lynch MA: **CD200 ligand receptor interaction modulates microglial activation in vivo and in vitro: a role for IL-4.** *J Neurosci* 2007, **27**:8309–8313.
  22. Chishti MA, Yang DS, Janus C, Phinney AL, Horne P, Pearson J, Strome R, Zuker N, Loukides J, French J, *et al*: **Early-onset amyloid deposition and cognitive deficits in transgenic mice expressing a double mutant form of amyloid precursor protein 695.** *J Biol Chem* 2001, **276**:21562–21570.
  23. Harris FM, Brecht WJ, Xu Q, Tesseur I, Kekoni L, Wyss-Coray T, Fish JD, Masliah E, Hopkins PC, Searce-Levie K, *et al*: **Carboxyl-terminal-truncated apolipoprotein E4 causes Alzheimer's disease-like neurodegeneration and behavioral deficits in transgenic mice.** *Proc Natl Acad Sci U S A* 2003, **100**:10966–10971.
  24. Nixon RA: **Autophagy, amyloidogenesis and Alzheimer disease.** *J Cell Sci* 2007, **120**:4081–4091.
  25. Ni Cheallaigh C, Keane J, Lavelle EC, Hope JC, Harris J: **Autophagy in the immune response to tuberculosis: clinical perspectives.** *Clin Exp Immunol* 2011, **164**:291–300.
  26. Mandrekar S, Jiang Q, Lee CY, Koenigsnecht-Talboo J, Holtzman DM, Landreth GE: **Microglia mediate the clearance of soluble Abeta through fluid phase macropinocytosis.** *J Neurosci* 2009, **29**:4252–4262.
  27. Harris J, De Haro SA, Master SS, Keane J, Roberts EA, Delgado M, Deretic V: **T helper 2 cytokines inhibit autophagic control of intracellular Mycobacterium tuberculosis.** *Immunity* 2007, **27**:505–517.
  28. Moscat J, Diaz-Meco MT: **p62 at the crossroads of autophagy, apoptosis, and cancer.** *Cell* 2009, **137**:1001–1004.
  29. Naert G, Laflamme N, Rivest S: **Toll-like receptor 2-independent and MyD88-dependent gene expression in the mouse brain.** *J Innate Immun* 2009, **1**:480–493.
  30. Herber DL, Mercer M, Roth LM, Symmonds K, Maloney J, Wilson N, Freeman MJ, Morgan D, Gordon MN: **Microglial activation is required for Abeta clearance after intracranial injection of lipopolysaccharide in APP transgenic mice.** *J Neuroimmune Pharmacol* 2007, **2**:222–231.
  31. Bolmont T, Haiss F, Eicke D, Radde R, Mathis CA, Klunk WE, Kohsaka S, Jucker M, Calhoun ME: **Dynamics of the microglial/amyloid interaction indicate a role in plaque maintenance.** *J Neurosci* 2008, **28**:4283–4292.
  32. Lee CY, Landreth GE: **The role of microglia in amyloid clearance from the AD brain.** *J Neural Transm* 2010, **117**:949–960.
  33. Liu Y, Walter S, Stagi M, Cherny D, Letiembre M, Schulz-Schaeffer W, Heine H, Penke B, Neumann H, Fassbender K: **LPS receptor (CD14): a receptor for phagocytosis of Alzheimer's amyloid peptide.** *Brain* 2005, **128**:1778–1789.
  34. Stewart CR, Stuart LM, Wilkinson K, van Gils JM, Deng J, Halle A, Rayner KJ, Boyer L, Zhong R, Frazier WA, *et al*: **CD36 ligands promote sterile inflammation through assembly of a Toll-like receptor 4 and 6 heterodimer.** *Nat Immunol* 2010, **11**:155–161.
  35. Hickman SE, Allison EK, El Khoury J: **Microglial dysfunction and defective beta-amyloid clearance pathways in aging Alzheimer's disease mice.** *J Neurosci* 2008, **28**:8354–8360.
  36. Majumdar A, Cruz D, Asamoah N, Buxbaum A, Sohar I, Lobel P, Maxfield FR: **Activation of microglia acidifies lysosomes and leads to degradation of Alzheimer amyloid fibrils.** *Mol Biol Cell* 2007, **18**:1490–1496.
  37. Paresce DM, Ghosh RN, Maxfield FR: **Microglial cells internalize aggregates of the Alzheimer's disease amyloid beta-protein via a scavenger receptor.** *Neuron* 1996, **17**:553–565.
  38. Bard F, Cannon C, Barbour R, Burke RL, Games D, Grajeda H, Guido T, Hu K, Huang J, Johnson-Wood K, *et al*: **Peripherally administered antibodies against amyloid beta-peptide enter the central nervous system and reduce pathology in a mouse model of Alzheimer disease.** *Nat Med* 2000, **6**:916–919.
  39. Colton CA, Mott RT, Sharpe H, Xu Q, Van Nostrand WE, Vitek MP: **Expression profiles for macrophage alternative activation genes in AD and in mouse models of AD.** *J Neuroinflammation* 2006, **3**:27.
  40. Veld BA I, Launer LJ, Hoes AW, Ott A, Hofman A, Breteler MM, Stricker BH: **NSAIDs and incident Alzheimer's disease. The Rotterdam Study [see comments].** *Neurobiol Aging* 1998, **19**:607–611.
  41. Sonnen JA, Larson EB, Walker RL, Haneuse S, Crane PK, Gray SL, Breitner JC, Montine TJ: **Nonsteroidal anti-inflammatory drugs are associated with increased neuritic plaques.** *Neurology* 2010, **75**:1203–1210.
  42. Golde TE, Miller VM: **Proteinopathy-induced neuronal senescence: a hypothesis for brain failure in Alzheimer's and other neurodegenerative diseases.** *Alzheimers Res Ther* 2009, **1**:5.
  43. Wyss-Coray T: **Inflammation in Alzheimer disease: driving force, bystander or beneficial response?** *Nat Med* 2006, **12**:1005–1015.
  44. Amor S, Puentes F, Baker D, van der Valk P: **Inflammation in neurodegenerative diseases.** *Immunology* 2010, **129**:154–169.
  45. Koenigsnecht-Talboo J, Landreth GE: **Microglial phagocytosis induced by fibrillar beta-amyloid and IgGs are differentially regulated by proinflammatory cytokines.** *J Neurosci* 2005, **25**:8240–8249.
  46. Shimizu E, Kawahara K, Kajizono M, Sawada M, Nakayama H: **IL-4-induced selective clearance of oligomeric beta-amyloid peptide(1–42) by rat primary type 2 microglia.** *J Immunol* 2008, **181**:6503–6513.
  47. Ong CT, Sedy JR, Murphy KM, Kopan R: **Notch and presenilin regulate cellular expansion and cytokine secretion but cannot instruct Th1/Th2 fate acquisition.** *PLoS One* 2008, **3**:e2823.
  48. Lee J, Chan SL, Mattson MP: **Adverse effect of a presenilin-1 mutation in microglia results in enhanced nitric oxide and inflammatory cytokine responses to immune challenge in the brain.** *Neuromolecular Med* 2002, **2**:29–45.

doi:10.1186/1750-1326-7-36

**Cite this article as:** Chakrabarty *et al*: Hippocampal expression of murine IL-4 results in exacerbation of amyloid deposition. *Molecular Neurodegeneration* 2012 **7**:36.

**Submit your next manuscript to BioMed Central and take full advantage of:**

- **Convenient online submission**
- **Thorough peer review**
- **No space constraints or color figure charges**
- **Immediate publication on acceptance**
- **Inclusion in PubMed, CAS, Scopus and Google Scholar**
- **Research which is freely available for redistribution**

Submit your manuscript at  
www.biomedcentral.com/submit

